Acta Pharmaceutica Sinica B 2020;10(6):1122−1133

Chinese Pharmaceutical Association
Institute of Materia Medica, Chinese Academy of Medical Sciences

Acta Pharmaceutica Sinica B

www.elsevier.com/locate/apsb
www.sciencedirect.com

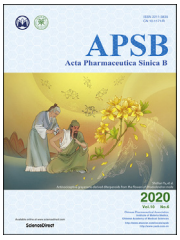

ORIGINAL ARTICLE

Interfacial properties and micellization of triblock poly(ethylene glycol)-poly(ε-caprolactone)-polyethyleneimine copolymers

Ji Li[a], Yitian Du[a], Haitao Su[a], Shixuan Cheng[a], Yanxia Zhou[a], Yiguang Jin[b,*], Xian-Rong Qi[a,*]

[a]*Key Laboratory of Molecular Pharmaceutics and New Drug Delivery System, School of Pharmaceutical Sciences, Peking University, Beijing 100191, China*
[b]*Department of Pharmaceutical Sciences, Beijing Institute of Radiation Medicine, Beijing 100850, China*

Received 4 July 2019; received in revised form 24 October 2019; accepted 11 November 2019

KEY WORDS

Block copolymers;
Langmuir films;
Molecular arrangement;
Self-assembly;
Nanostructure

Abstract This study aimed to explore the link between block copolymers' interfacial properties and nanoscale carrier formation and found out the influence of length ratio on these characters to optimize drug delivery system. A library of diblock copolymers of PEG-PCL and triblock copolymers with additional PEI (PEG-PCL-PEI) were synthesized. Subsequently, a systematic isothermal investigation was performed to explore molecular arrangements of copolymers at air/water interface. Then, structural properties and drug encapsulation in self-assembly were investigated with DLS, SLS and TEM. We found the additional hydrogen bond in the PEG-PCL-PEI contributes to film stability upon the hydrophobic interaction compared with PEG-PCL. PEG-PCL-PEI assemble into smaller micelle-like (such as PEG-PCL4006-PEI) or particle-like structure (such as PEG-PCL8636-PEI) determined by their hydrophilic and hydrophobic block ratio. The distinct structural architectures of copolymer are consistent between interface and self-assembly. Despite the disparity of constituent ratio, we discovered the arrangement of both chains guarantees balanced hydrophilic−hydrophobic ratio in self-assembly to form stable construction. Meanwhile, the structural differences were found to have significant influence on model drugs

Abbreviations: AFM, atomic force microscope; A_{min}, critical molecular area; CMC, critical micelle concentration; DLS, dynamic light scattering; DTX, docetaxel; GPC, gel permeation chromatography; LB, Langmuir−Blodgett; N_{agg}, polymer aggregation number; Np, nano-assembly numbers; PCL, poly(ε-caprolactone); PDI, polydispersity; PEG, poly(ethylene glycol); PEI, polyethyleneimine; R_g, gyration radius; R_h, hydrodynamic radius; SLS, static light scattering; TEM, transmission electron microscope

*Corresponding authors. Tel./fax: +86 10 82801584.
E-mail addresses: jinyg@sina.com (Yiguang Jin), qixr@bjmu.edu.cn (Xian-Rong Qi).

Peer review under responsibility of Institute of Materia Medica, Chinese Academy of Medical Sciences and Chinese Pharmaceutical Association.

https://doi.org/10.1016/j.apsb.2020.01.006

incorporation including docetaxel and siRNA. Taken together, these findings indicate the correlation between molecular arrangement and self-assembly and inspire us to tune block compositions to achieve desired nanostructure and drug loading.

1. Introduction

In recent years, block copolymers have attracted an increasing research interest, due to their wide application in the field of soft materials[1], diagnosis and imaging[2], water purification[3], biomaterials[4], and drug delivery systems[5,6]. Amphiphilic copolymers have the potential to self-assemble in selective solvent and interface, which leads to various nanostructures and morphologies such as micelles, vesicles, rods, and particles. They have been extensively explored both theoretically and experimentally to understand their interfacial arrangement and self-organization nanostructures at the air/water interface[7,8] and in bulk[9,10].

Langmuir monolayer measurement is a useful technique for the interfacial property studies of amphiphilic small molecules[11,12], block copolymers[7,8] and biomacromolecule[13,14]. Block copolymers have the ability to form the monolayer at the air/water interface, *i.e.*, hydrophilic blocks submerge into the subphase and hydrophobic blocks anchor at the interface. During compression, surface pressure is measured as a function of the mean molecular area (π−A isotherms or Langmuir isotherms). The polymeric isotherms deal with intermolecular forces and molecular arrangement in two-dimensional space and indicate the various phases corresponding to the transitions of copolymer chains[15]. Thus, the isotherm can provide information about molecular packing. It is also widely used to determine interfacial properties of copolymers. These characters have been found to be influenced by the conformation of polymeric chains and hydrophilic/hydrophobic properties of copolymers[16] and are important to affect their biological activities and applications. Thus measurement of polymeric π−A isotherms provide useful information on static/dynamic properties of the copolymer chains to further guide their self-assembly in solution.

Poly(ethylene glycol)-poly(ε-caprolactone) block copolymers (PEG-PCL) approved by U. S. Food and Drug Administration (FDA) have been applied as drug delivery system due to their brilliant biocompatibility and degradability[17]. Its hydrophobic PCL chain spontaneously self-assembles into an inner core loading hydrophobic drugs and surrounded by hydrophilic PEG corona in medium. Additionally, polyethylenimine (PEI) has gained much more attention recently because of abundant amines to condense gene drugs and facilitate endosomal escape[18]. In the current study, we are expecting to extend fundamental investigation to a series of triblock copolymers PEG-PCL-PEI based on the former studies about PEG-PCL and PEI-PCL. Triblock copolymers contain more segments, in which all constituents have distinct chemical and physical properties. They can form a variety of nanostructures in solution by controlling assembly conditions, segments ratios, and blocks composition[19]. However, self-assembly of triblock copolymers for drug delivery is often empirical. The lack of rational and delicate tune results in poor reproducibility and controllability. Triblock copolymers composed of poly(ethylene oxide) (PEO), poly(propylene oxide) (PPO) and polystyrene (PS) have been extensively studied[20,21], but similar PEG-PCL-PEI have gained less exploration. The potential to use the resulting self-assembled PEG-PCL-PEI for developing drug delivery system has motivated us to put forward related research. The increasing need for filling the aforementioned deficiency sets the foundation for this research.

In the present study, we investigate the interfacial behavior of PEG-PCL-PEI triblock copolymers with varying PCL lengths and constant copolymerization of PEG and PEI chains with a guide toward drug encapsulation and delivery. Firstly, systematic studies of Langmuir films help us to know surface properties and molecular arrangement of copolymers. Furthermore, we investigate whether these triblock copolymers can develop a drug delivery system for nucleic acids and hydrophobic chemotherapeutic drugs. Self-assembly of copolymers was examined by dynamic light scattering (DLS), static light scattering (SLS) and transmission electron microscope (TEM). A molecular-level understanding of the interface properties and copolymer chain conformations are crucial to build fundament for the well-control biological application of the nano-assemblies. To this end, our research efforts have concentrated on understanding the link between hydrophilic/hydrophobic compositions of copolymers and interfacial properties, self-assembly nanostructures including size, morphology and drug encapsulation. Our results indicate block length ratio and hydrophilic/hydrophobic properties have an important impact on surface properties and assembly formation. It is useful to guide block constitute selection and certain drug carrier forming for better drug encapsulation and transport. Well-controlling delicate balance of hydrophilic/hydrophobic length ratio can optimize self-assembly and applications in drug delivery.

2. Materials and methods

2.1. Materials

PEG_{1900}, PEI_{2500} and DNA were purchased from Sigma−Aldrich (St. Louis, MO, USA). Docetaxel (DTX) was obtained from Norzer Pharmaceutical Co., Ltd. (Beijing, China). The scrambled siRNAs were purchased from Genepharma (Shanghai, China). All other reagents and chemicals were analytical grade.

2.2. Synthesis and characterization of copolymers

The diblock PEG-PCL and triblock PEG-PCL-PEI copolymers were synthesized as described previously[22,23] with minor modifications. Briefly, PEG (macroinitiator), caprolactone (amounts calculated to the designated PCL lengths) and $Sn(Oct)_2$ (catalyst; 0.1%, mol/mol, corresponding to caprolactone) were put into a reaction flask with methylbenzene as solvent and purged with dry

nitrogen. Subsequently, the reaction was carried out at a temperature of 115 °C for 24 h. After removing methylbenzene by rotary evaporation, PEG-PCL product was purified by third precipitating into cold methanol from dichloroform, and finally vacuum-dried.

Then the end chain of PCL was modified with a double bond using acryloyl chloride. PEG-PCL diblock copolymers were mixed with 1.00 eq. of triethylamine and 2.00 eq. acryloyl chloride dissolved in benzene and reacted for 12 h reflux at 80 °C. After removing $NHEt_3Cl$ crystallization by filtration, the product PEG-PCL-linker precipitated in cold hexane as above.

Conclusively, PEI was coupled onto PEG-PCL-linker copolymer by Michael addition reaction. 1.00 eq. of PEI and 1.00 eq. PEG-PCL-linker were added into separate reaction flasks and dried. After purging with nitrogen, PEG-PCL-linker was dissolved in chloroform, while PEI in methanol. The PEI containing flask was heated to 60 °C and then PEG-PCL-linker was added dropwise. The reaction mixture was stirred at 60 °C for 24 h. The obtained product PEG-PCL-PEI purified by precipitation in cold diethyl ether.

The chemical structure of copolymers dissolved in D_2O was determined by ^1H NMR analysis (400 MHz, AVANCE III 400, Bruker Inc., Karlsruhe, Germany). Gel permeation chromatography (GPC, 1515 GPC HPLC, Waters Corporation, Milford, MA, USA) which includes 2410 differential refraction detector and Waters 515 pump was used to determine the copolymers' number-average molecular weight (Mn), weight-average molecular weight (Mw) and polydispersity (PDI). A solution of tetrahydrofuran (HPLC grade) was used as eluent (0.5 mL/min) and 100 μL copolymer samples at appropriate concentrations were injected for each measurement. A series of poly(methyl methacrylate) standards were used as a calibration curve.

2.3. Langmuir monolayer and surface pressure measurement

The π−A isotherms of copolymers were measured using a Minitrough II film balance (KSV, Finland) equipped with dual barriers and a Pt Wilhelmy plate-sensing device at a temperature of 25 °C. The Teflon trough has a width of 75 mm and the area of 24,300 mm^2. The subphase was purified water of 18 MΩ. A predetermined copolymer solution (0.1 mg/mL for diblock copolymers and 0.2 mg/mL for triblock copolymers) in chloroform was prepared and deposited onto the subphase using a microsyringe. To obtain complete surface pressures isotherm, each copolymer was spread at different initial volumes ranging from 20 to 50 μL, leading to different initial pressures. The different parts of isotherm were first recorded and then combined into one plot, and thus overlapped within the experimental error. Compression was initiated after a delay of 15 min allowing chloroform evaporation to ensure no residual organic solvent. The compression rate was 5 mm/min.

The deformability of triblock copolymers was determined by static modulus and dynamic modulus. The procedure was the same as π−A isotherm measurement. When achieving the designated pressure, barriers stopped moving. The damping curve of surface pressure as a function of time (namely static modulus) was recorded. As for dynamic modulus, keep barriers vibration at constant frequency along the trough at designated pressure. The typical vibration curves of surface pressure as a function of time was recorded indicative dynamic stability of the film.

2.4. Critical micelle concentration (CMC)

The CMC of copolymers was measured by fluorescence method using pyrene[24]. The pyrene solution (0.1 mg/mL, 50 μL) in acetone was prepared and added to the test tubes. After removing acetone by air-dry, a series of copolymer solutions at different concentrations were added while the concentration of pyrene in each solution was fixed at 6×10^7 mol/L and then the mixture was shaken at room temperature for 24 h in dark. Fluorescence detection was set up with an emission wavelength of 330 nm, and excitation spectra were scanned between 300 and 400 nm. The ratio of fluorescence intensity at 373 and 384 nm (I_{384}/I_{373}) was calculated and plotted against the negative logarithm of the concentration of copolymers. The intersection of two linear regressions was considered as CMC value.

2.5. Self-assembly of block copolymers and drug loading

The nano-assemblies were prepared using film-hydration method[25]. Briefly, copolymers were dissolved in chloroform/methanol (3:1, *v*/*v*) at concentrations ranging from 1−20 mg/mL into a pear-shaped flask and subsequently evaporated to form a dry film using a rotary evaporator under vacuum at 40 °C. Then the dried film was hydrated to obtain blank-assembly.

DTX-loaded assembly was prepared at DTX and copolymers of 1:10 (*w*/*w*) by film-hydration method. The dispersion was filtered through a 0.22 μm film to remove free DTX. The amount of DTX in assembly was determined by HPLC system with a UV detector (LC-20AT pump, SPD-20A UV detector, Shimadzu, Japan). A Diamonsil reverse-phase C18 column (250 mm × 4.6 mm, pore size 5 μm) was used for analysis. The mobile phase consisted of acetonitrile and water (57/43, *v*/*v*). Flow rate is 1.0 mL/min and the detection wavelength was set at 230 nm. All samples were analyzed in triplicate.

For siRNA-loaded assembly, equal volume of blank-assembly and siRNA stock solution were mixed together by vortex, and followed incubating for 30 min at room temperature. Agarose gel electrophoresis was carried out to determine the siRNA condensation abilities. The complexes were electrophoresed for 10 min at 120 V in TBE buffer on a 1% (*w*/*v*) agarose gel containing 0.5 μg/mL ethidium bromide. The electrophoretic mobility was visualized on a UV illuminator. Heparin competition study was used to examine the stability of siRNA-loaded assembly. Different amounts of heparin (heparin:siRNA = 0.1, 0.5, 1, 2, 4, 8, 12, and 20; *w*/*w*) were added into siRNA-loaded assembly (*N*/*P* = 10/1) and then incubated for another 30 min and subsequently analyzed by agarose gel mobility assay[26].

2.6. Dynamic light scattering (DLS), static light scattering (SLS) and transmission electron microscopic (TEM)

The size, polydispersity index (PDI) and zeta-potential of all assemblies were measured by DLS using a Zetasizer Nano ZS (Malvern Instruments Ltd., Worcestershire, UK). All samples were carried out in triplicate.

R_g (gyration radius), Mw (molecular weight) and N_{agg} (aggregation number) of assemblies were detected by SLS. A commercialized spectrometer (Brookhaven Instruments Co., Holtsville, NY, USA) equipped with a 100 mW solid-state laser (GXC-III, CNI, Changchun, China) operating at 632 nm was used to conduct SLS experiments. Photon correlation measurements in self-beating mode were carried out at multiple scattering angles by using a Digital Correlator.

Transmission electron images were obtained using a JEM-200CX (Jeol, Tokyo, Japan). After dilution with distilled water, droplets of the dispersions were placed on the surface of a

formvar-coated copper grid, followed by a negative staining using uranyl acetate solution (1%, *w*/*v*), and air-dried overnight at room temperature.

2.7. Statistical analysis

All values are expressed as mean ± standard deviation (SD). Statistical analysis was performed using standard Student's *t*-test or one-way analyses of variance (ANOVA).

3. Results

3.1. Synthesis and characterization of copolymers

A series of PEG-PCL diblock copolymers and PEG-PCL-PEI triblock copolymers were synthesized (Supporting Information Scheme S1). PEG-PCL was synthesized by ring-open copolymerization. Through changing feed ratio of caprolactone, we obtained a library of diblock copolymers with varying PCL segments (from 600 to 8636) and fixed copolymerization of PEG. Then, the PEG-PCL was terminated with a double bond by reacting with acryloyl chloride. PEI-PCL-PEG was synthesized by coupling the PEI to PEG-PCL-linker through the Michael-type addition reaction.

The characteristics of the diblock copolymers and derived triblock copolymers are shown in Table 1. The molecular weight of PEG-PCLs calculated from the ^{1}H NMR (400 MHz, $CDCl_3$) spectra (Supporting Information Fig. S1) was approximately the same as GPC, also consistent with theoretical molecular weight. The PDI of all PEG-PCLs was less than 1.22, indicating the narrow distribution. Through direct and mild synthesis route, we can easily control the molecular weight of copolymers and get the product by convenient precipitation.

3.2. π−A isotherms and molecular behaviors at air/water interface

Interfacial properties of amphiphilic block copolymers were studied at the air/water interface by surface pressure measurements. The isotherms of PEG-PCL diblock copolymers (Fig. 1A) and PEG-PCL-PEI triblock copolymers (Fig. 1B) revealed that the lengths of constituent blocks had a major effect on their interfacial behavior. The inflection point in Langmuir isotherms that is usually indicative of phase transitions, was distinguished from film compressibility (*Cs*) *versus* surface pressure, *i.e* [$Cs = -1/A \times (dA/d\pi)$], which resulting in local maxima in isothermal compressibility that correspond to conformational rearrangements[27], as shown in Supporting Information Figs. S2A and S2B for diblock and triblock copolymers respectively.

Critical molecular areas (A_{min}) corresponded to limiting area prior to collapse by extrapolation the tangent to maximum slope of the isotherm. The A_{min} of diblock copolymers as well as triblock copolymers increased almost linearly with PCL length indicating the molecular behavior at this regime mainly resulted from steric interactions between hydrophobic PCL blocks (Supporting Information Fig. S3). The triblock copolymers had obviously smaller A_{min} (Table 2) and higher kink point (indicate film collapse, Fig. 1) than corresponding diblock copolymers. This meant the PEG-PCL-PEI may have special interactions that contributed to a more stable arrangement.

Usually, the proposed molecular arrangements of diblock copolymer are shown in Fig. 2A. At the beginning, the molecules were separated at the surface and adopted flattened conformation (pancake). As the pressure increased, the pancake pattern changed to a brush pattern (where hydrophilic chains submerged into water and hydrophobic chains anchored at the interface) and further compression led to molecular overlap until collapse[27] (phase transitions were indicated by maxima in Fig. S2A). For the PEG-PCL-PEI, the isotherms and compressibility plots suggested that one hydrophilic segments of triblock copolymer entered the subphase and the other stretched away from the interface alternately and supported by intermediate PCL chains (Fig. 2B). This pattern allowed the triblock copolymer condensed well due to the hydrogen bonding beyond van der Waal interactions between neighboring PEI and PEG chains, thus bringing brought small A_{min}. The hydrogen bonds are pronounced as primary non-covalent driving force to bolster molecular arrangement and stabilize aggregate formation[28].

Beyond that, a new phase transition at 35 mN/m only for PEG-PCL8636-PEI could be visualized (Fig. S2B), demonstrating some type of special organization that was absent for other triblock copolymers. It was speculated that long flexible PCL was not sufficient to support its vertical arrangement at lower surface pressure. PEG-PCL8636-PEI adopted intermediate state (Fig. 2C) where two hydrophilic segments contacted with water and further compression led to loop formation of hydrophobic PCL chains. The chain folding is a common structure for block copolymers and

Table 1 Characteristics of the diblock copolymers and derived triblock copolymers.

Diblock copolymer	PEG:PCL	Molecular weight of PEG-PCL				PDI[d]	Triblock copolymer
PEG_{1900}-PCL*x*[e]	Weight ratio	Theoretical[a]	^{1}H NMR[b]	Mw[c]	Mn[c]		PEG_{1900}-PCLx-PEI_{2500}[e]
PEG-PCL600	1:0.5	2850	2613	2800	2500	1.12	PEG-PCL600-PEI
PEG-PCL1947	1:1	3800	3764	4077	3847	1.06	PEG-PCL1947-PEI
PEG-PCL2945	1:1.5	4750	4625	5717	4845	1.18	PEG-PCL2945-PEI
PEG-PCL4006	1:2	5700	5698	7086	5906	1.20	PEG-PCL4006-PEI
PEG-PCL4826	1:2.5	6650	6632	6995	6726	1.04	PEG-PCL4826-PEI
PEG-PCL5930	1:3	7600	8019	8613	7830	1.10	PEG-PCL5930-PEI
PEG-PCL8636	1:4	9500	9974	12854	10536	1.22	PEG-PCL8636-PEI

[a]Theoretical molecular weight was calculated by the feed ratio.
[b]^{1}H NMR molecular weight was calculated by the ^{1}H NMR spectroscopy (Bruker).
[c]Mw and Mn were determined by GPC measurements (Waters).
[d]PDI = Mw/Mn.
[e]*x* presented the Mn of PCL block if not specified.

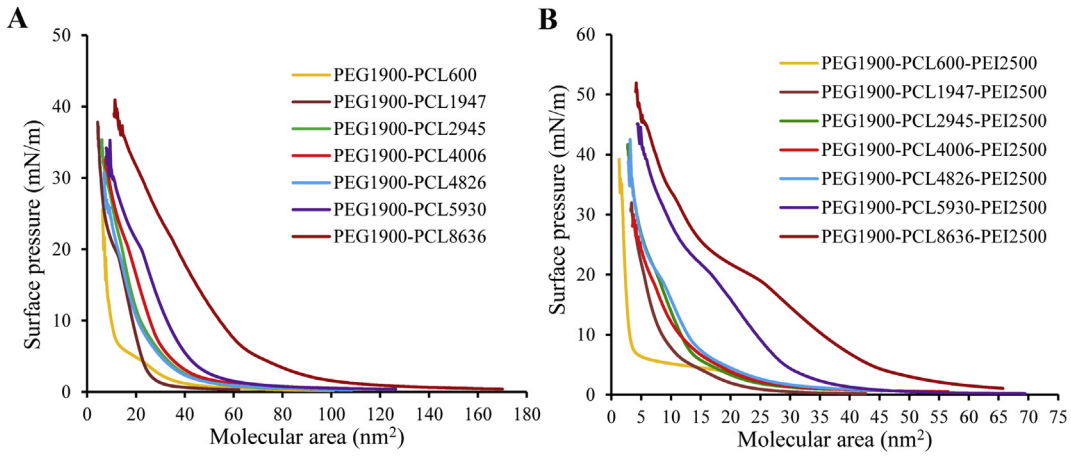

Figure 1 Langmuir isotherms for spread film of PEG-PCL diblock copolymers (A) and PEG-PCL-PEI triblock copolymers (B) at 25 °C.

this phenomenon is gradually produced with the continuous change of length of PCL chains, not a discrete transition. Until 35 mN/m, a point was reached when one of hydrophilic chains was repelled out of water. After this, PEG-PCL8636-PEI changed conformation from transitional arrangement to vertical state for better film stability. This phenomenon, which one of the two-end hydrophilic group was removed from subphase, is well established and reported[15,29,30], particularly for the amphiphile with relatively longer hydrophobic lengths.

To investigate our speculations about the molecular arrangement, we first observed morphologies of copolymer films by atomic force microscope (AFM, SPA 400, Seiko Instruments Inc., Tokyo, Japan) using Langmuir−Blodgett (LB) deposition shown in Supporting Information Fig. S4. PEG-PCL1947-PEI (Fig. S4A) and PEG-PCL4006-PEI (Fig. S4B) presented a flat surface at lower pressures but depicted some brighter micro-domains[15] at 25 mN/m because of vertical ordering chains. As for PEG-PCL8636-PEI, Fig. S4C shows more continuous and smoother layer and still to 25 mN/m, the spread of molecules was more packed rather than forming micro-domain. The reason was that PEG-PCL8636-PEI at intermediate state could form more homogeneous matrix because of most PCL chains surface occupation. The differences between AFM images of triblock copolymers resulted from their discrepancy in molecular arrangement. Furthermore, we employed PBS with different pH values (7.4, 6.5, and 5.5) and DNA solution as the subphase to verify molecular arrangement of block copolymer at interface. Lowering the pH value from 7.4 to 5.5 increases the protonation of PEI just like the proton sponge effect in the endosome[31]. It can be seen from Supporting Information Fig. S5A, the isotherms almost superposed from pH 7.4 to 5.5 for PEG-PCL1947-PEI and PEG-PCL4006-PEI because the hydrogen-bonding complexation between the PEI and the PEG forms very compact layers to compromise the more protonated PEI[32]. However, the isotherms of PEG-PCL8636-PEI were nearly identical at lower pH values (5.5 and 6.5), but different from that at 7.4. Relative to others, PEG-PCL8636-PEI had more PEI molecules into the water at intermediate state (Fig. 2C), more repulsive interactions at lower pH values resulting in increased surface occupancy and not condensed well monolayers[11]. Then DNA solution was used as subphase to introduce an electrostatic absorption between PEI chains and negative DNA. Fig. S5B shows the isotherms of PEG-PCL1947-PEI and PEG-PCL4006-PEI occupied more areas in DNA solution (increased $A_{min,}$ Table 2). This behavior was interpreted that two hydrophilic chains of above copolymers may both submerged into water due to attraction of DNA. Meanwhile, the isotherms of PEG-PCL8636-PEI almost stayed the same whenever the subphase was. This precisely showed absorbed DNA stabilized film (decreased A_{min}, Table 2) instead of changing its intermediate state.

Given the basis of molecular arrangement above, the deformability of triblock copolymers was determined by the static modulus and dynamic modulus[33]. Supporting Information Fig. S6A shows surface pressure of PEG-PCL8636-PEI at 25 mN/m dropped evidently compared to two others. At this pressure, PEG-PCL1947-PEI and PEG-PCL4006-PEI formed stable monolayer due to the hydrogen bond, whereas PEG-PCL8636-PEI in intermediate state led to inevitable tension decrease. Then dynamic modulus presented in Fig. S6B demonstrated the tension of

Table 2 The A_{min} (nm^2) of corresponding diblock copolymers and triblock copolymers in water and in DNA solution.

Molecular weight of PCL chains	In water		In DNA solution
	Diblock copolymer	Triblock copolymer	Triblock copolymer
PCL600	14.47	3.00	–
PCL1947	14.16	8.76	13.39
PCL2945	25.04	8.08	–
PCL4006	29.58	14.55	19.03
PCL4826	32.16	17.52	–
PCL5930	40.62	20.66	–
PCL8636	62.16	29.93	25.10

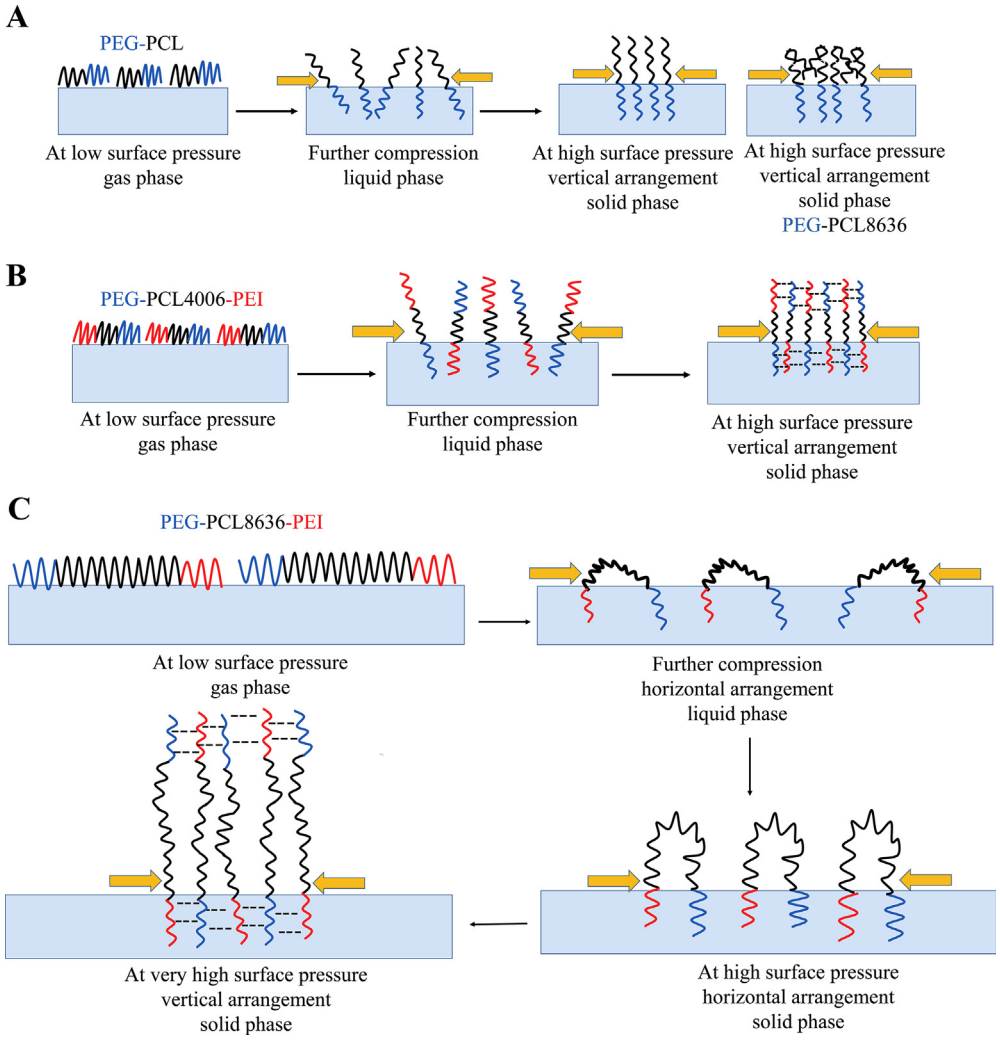

Figure 2 Proposed molecular arrangement of diblock copolymer (A) and triblock copolymer (B) at the air/water interface, where PEG-PCL4006-PEI as a typical presentation. Hydrogen bond between neighboring PEI chains and PEG chains contributes to stabilization of triblock copolymers. When the PCL is long as 8636, the copolymer has intermediate state where two hydrophilic chains contact with water surface and changes conformation to vertical state at high pressure (C).

PEG-PCL8636-PEI presented obvious attenuation, whereas PEG-PCL1947-PEI and PEG-PCL4006-PEI still maintained their own state. Overall, the longest PCL chains of PEG-PCL8636-PEI owned better deformability and could not support its vertical arrangement at lower surface pressure so that intermediate state existed. These results were in great agreement with our previous study about the molecular arrangement.

3.3. Nano-assemblies and assembly mechanism of block copolymers

Using film balance technique, surface properties of block copolymers had been investigated. In the next step, we developed the amphiphilic block copolymers into nano-assemblies for delivering antitumor chemotherapeutic and genetic drugs. To rationally design and tune, it is necessary to study the amphiphilic copolymers assembling into carriers about their structure, nano-size, drug encapsulation and stability.

At first, the fluorescent probe method was used to measure the critical micelle concentration (CMC) of different copolymers (Supporting Information Fig. S7). The CMC values of PEG-PCL4006, PEG-PCL8636, PEG-PCL4006-PEI and PEG-PCL8636-PEI were 1.39×10^{-7}, 5.74×10^{-7}, 1.54×10^{-6} and 2.39×10^{-6} mol/L, respectively. Notably, the CMC values of these copolymers depend on the copolymer composition and block ratio[34]. Such low CMC values guaranteed these block copolymers self-assemble into nano-scaled carriers with desired stability[34], considering the dilution upon injection.

Based on the meaningful CMC, nano-assemblies were prepared using the most common film-hydration method. The size (hydrodynamic diameter), polydispersity index (PDI) and zeta-potential of all nano-assemblies were measured by DLS (Supporting Information Fig. S8). For diblock copolymers (Fig. 3A and Supporting Information Table S1), blank assemblies of PEG-PCL600 and PEG-PCL8636 had relatively large diameters above 200 nm and PDIs were close to 0.3, which may result from their wide disparity of hydrophilic and hydrophobic chains. The other five diblock copolymers were capable to self-assemble into polymeric micelles[35] as shown in Fig. 4A, which sizes were less than 50 nm with small PDIs in a range of 0.137−0.184 and zeta

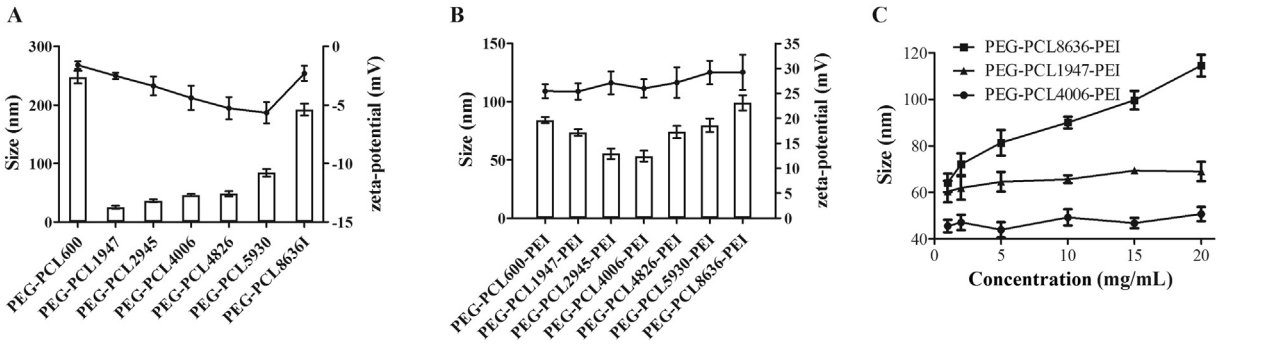

Figure 3 Hydrodynamic diameters (column) and zeta potential (line) of blank diblock copolymers assemblies (A) and blank triblock copolymers assemblies (B). Size of assemblies as a function of initial copolymer concentration in the film-hydration process (C). All data are monitored by DLS (Zetasizer Nano ZS, Malvern Instruments Ltd.) and data are presented as mean ± SD for at least three different preparations.

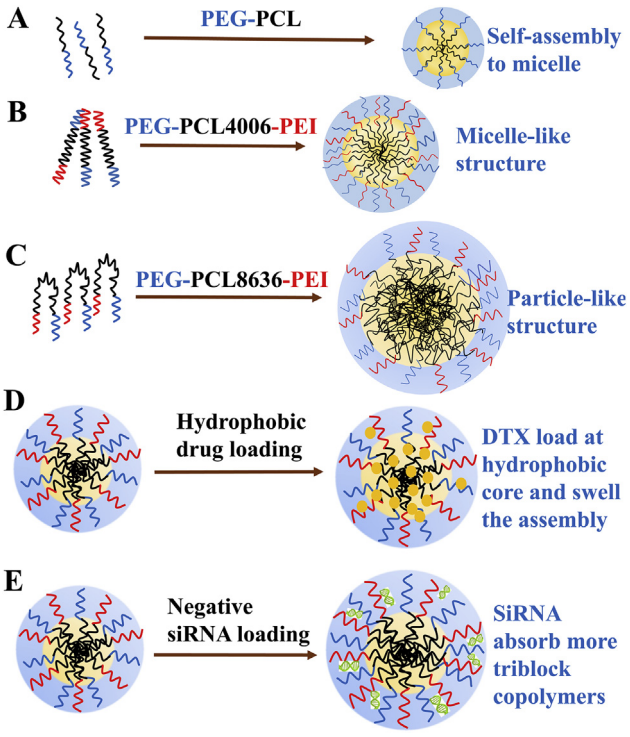

Figure 4 Sketches of assemblies. Diblock copolymers PEG-PCL assemble to small micelles (A). PEG-PCL4006-PEI forms micelle-like assemblies (B). PEG-PCL8636-PEI forms particle-like assemblies (C). DTX loaded at the hydrophobic core to swell the structure consequently increasing size (D). The siRNA absorbed on the outer shell to re-assemble a new gene vector (E).

potentials were −1 to −6 mV. Importantly, the micelles of PEG-PCL1947 had the smallest size, due to balanced hydrophilic and hydrophobic chains.

Fig. 3B and Supporting Information Table S2 show all triblock copolymers can form nano-assemblies with diameters ranging from 53 to 99 nm and acceptable size distribution (PDI in a range of 0.133−0.225). All assemblies were positively charged [about +(25−29) mV] due to the presence of PEI. The zeta potentials did not change significantly because of same copolymerization of PEG and PEI. The hydrophilic PEG shells shielding of PEI charges by shifting the slipping plane away from the surface of the PCL core determined the zeta-potential of nano-assemblies[22]. In particular, assemblies of PEG-PCL4006-PEI had the smallest size, mainly due to their fair hydrophilic/hydrophobic ratio.

The size of assembly as a function of copolymer concentration was measured to explain assembly mechanism and nanostructure. As revealed by Fig. 3C, the size of PEG-PCL1947-PEI and PEG-PCL4006-PEI assemblies kept nearly constant during copolymers concentration increasing, however, assemblies sizes expanded with higher PEG-PCL8636-PEI concentrations implying a different formation process.

To elucidate assembly formation, we operated SLS to monitor the change of copolymer aggregation numbers (N_{agg}) and nano-assembly numbers (N_p) as a function of copolymer concentration (Table 3). With increasing copolymer concentration, PEG-PCL1947-PEI and PEG-PCL4006-PEI could form more nano-assemblies (N_p is growing) whereas N_{agg} only increased slightly implying less size change (Fig. 3C). Whereas, higher concentrations for PEG-PCL8636-PEI generated larger nano-assembles (increasing N_{agg} and sizes), but N_p increase slightly. These findings indicated that PCL chains in PEG-PCL8636-PEI aggregated quickly upon water phase forming particle-like structures. The PCL folded in the core resulting in a reduction of corona chain crowding, thus forming dense core and thin shell (Fig. 4C). The longest PCL chains agglomerated into compact cores with a high curvature, just like intermediate state at the interface (Fig. 2C). Whereas relatively longer hydrophilic segments of PEG-PCL1947-PEI and PEG-PCL4006-PEI prevented PCL chains quickly association and controlled assembly formation leading to smaller micelle-like structures (Fig. 4B), independence of size over the copolymer concentration (Fig. 3C). These micellar assemblies are composed of linear polymeric chains consistent with interfacial arrangement (Fig. 2B), which have thick shell and loose core.

3.4. *Drug encapsulation and morphology observation*

It has known size and structure of blank assemblies influenced by length ratio of blocks. We then chose DTX (Norzer Pharmaceutical Co., Ltd.) and siRNA (Genepharma) as representing hydrophobic and electrostatic interaction to compare loading capacities of different triblock copolymers. The sizes of DTX-loaded assemblies slightly increased 8−17 nm corresponding to blank ones (Fig. 3B and Supporting Information Table S2) with unchangeable positive charge (Fig. 5A and Supporting Information Table S3). It is most likely DTX dissolved into hydrophobic core (Fig. 4D),

Table 3 Static light scattering (SLS) parameters of assemblies formed by PEG-PCL1947-PEI, PEG-PCL4006-PEI, PEG-PCL8636-PEI in different concentrations.

	Concentration (mg/mL)	Mw (g/moL)	N_{agg}	N_p ($\times 10^{15}$)
PEG-PCL1947-PEI	2	434100	68.1	2.70
	10	466600	73.2	12.8
	20	492710	77.3	24.0
PEG-PCL4006-PEI	2	475800	56.6	2.50
	10	539600	64.2	11.1
	20	583400	69.4	20.6
PEG-PCL8636-PEI	2	1013000	77.7	1.18
	10	4390150	336	1.37
	20	7921000	607	1.52

maintained its outer positive charge but swelled the sizes slightly. PEG-PCL1947-PEI and PEG-PCL4006-PEI showed good loading capacities for DTX, 83.6%−85.6% determined by HPLC system (Supporting Information Table S4, Shimadzu), maybe due to the self-assembly composed of linear polymeric chains with more accessible volume for drug loading[36]. Nevertheless, PEG-PCL8636-PEI showed less encapsulation efficiency of 78.7%, presumably originating from high core density comprised of folded PCL chains (Fig. 4C), thus leaving no enough space for drug incorporation[37,38].

Condensation capability is primary for cationic copolymer-based gene delivery system. As shown in Supporting Information Fig. S9, triblock copolymers can condense siRNA well at and above *N*/*P* ratio of 8/1 where nearly no free siRNA was detected. Based on the electrophoresis result, we chose *N*/*P* ratio of 10/1 to prepare following siRNA-loaded assemblies.

After complexing with siRNA, assemblies' sizes increased 32−45 nm (Fig. 5B and Supporting Information Table S5) compared to blank assemblies (Fig. 3B and Supporting Information Table S2), and naturally, zeta-potentials declined from approximately +27 to +(6.6−9.6) mV. These results revealed negative siRNA absorbed in the outer corona, neutralized a portion of positive PEI and expanded assemblies size, as presented in Fig. 4E.

The PEG-PCL-PEI can protect siRNA against nucleases degradation[39] in serum or cytoplasm. Here to investigate impact of copolymer/siRNA ratio on assembly, we added siRNA continuously to achieve specific *N*/*P* ratio to study size and zeta-potential changes (Supporting Information Fig. S10). Compared to blank ones, the sizes of all complexes decreased when small amounts of siRNA (*N*/*P* = 50:1 for PEG-PCL1947-PEI and PEG-PCL4006-PEI, *N*/*P* = 30:1 for PEG-PCL8386-PEI) was added, followed by gradually growing. The different turning points proved their differences in structure and related binging capacity. Furthermore, different amounts of heparin as competitive replacement of siRNA were added to investigate anti-anion stability[40]. Fig. 5C depicts that PEG-PCL1947-PEI and PEG-PCL4006-PEI began to dissociate siRNA when heparin/siRNA weight ratio is over 0.5. However, PEG-PCL8636-PEI were more protective against heparin because they leaked out siRNA when ratio over 4. On one hand, micellar assemblies comprised of linear chains had larger available area per PEI chains, leading to more dynamic heparin

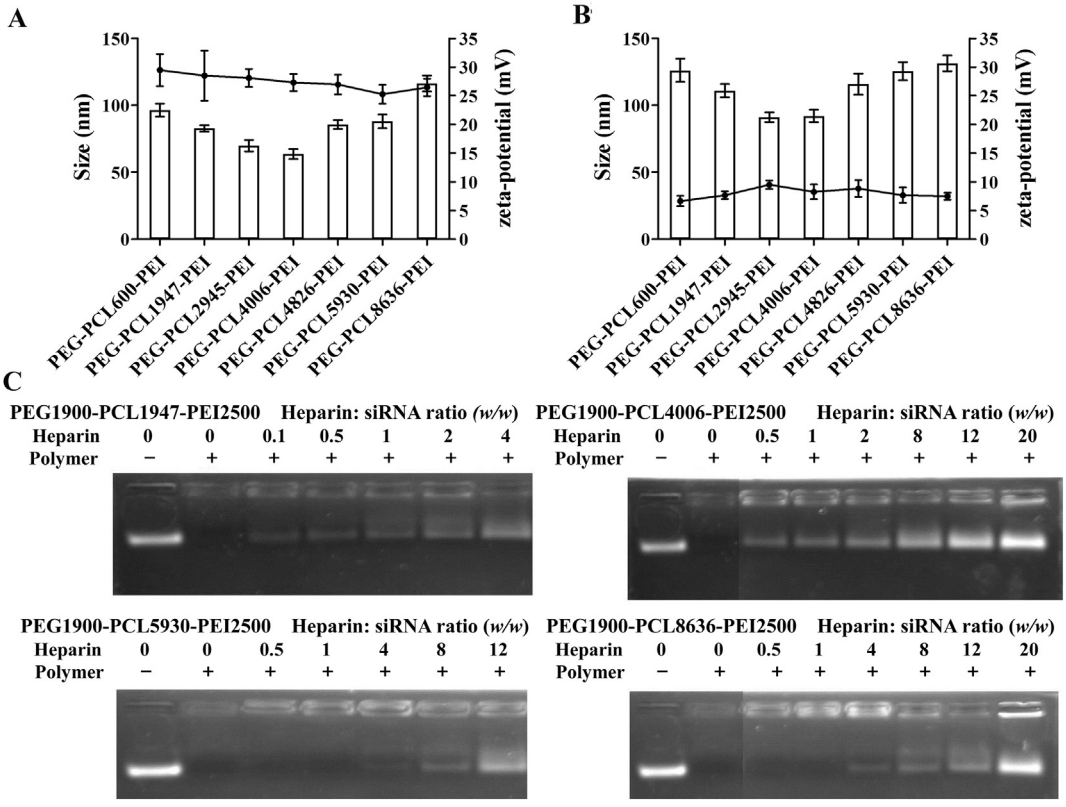

Figure 5 Hydrodynamic diameters (column) and zeta potential (line) of DTX loaded-assemblies (A) and siRNA loaded-assemblies (B). Heparin competitive replacement to investigate anti-anion stability, lane numbers were corresponded to different weight ratio of heparin to siRNA (*w*/*w*) (C). All data in (A) and (B) are monitored by DLS and data are presented as mean ± SD for at least three different preparations.

Table 4 Static light scattering (SLS) parameters of different assembly preparations.

Preparation	R_h (nm)	R_g (nm)	R_g/R_h	Mw (g/mol)	N_{agg}
PEG-PCL1947-PEI	36.99	41.62	1.125	434100	68.1
PEG-PCL4006-PEI	26.98	28.49	1.056	475800	56.6
PEG-PCL5930-PEI	38.17	44.20	1.158	922400	89.3
PEG-PCL8636-PEI	47.44	54.74	1.154	1013000	77.7
PEG-PCL1947-PEI/DTX	42.56	48.12	1.121	256170	51.0
PEG-PCL4006-PEI/DTX	31.08	32.07	1.032	255300	49.2
PEG-PCL5930-PEI/DTX	45.07	51.69	1.147	432900	73.3
PEG-PCL8636-PEI/DTX	57.68	65.53	1.136	401000	62.8
PEG-PCL1947-PEI/siRNA	62.05	63.54	1.024	697100	84.6
PEG-PCL4006-PEI/siRNA	45.07	44.98	0.998	745300	68.5
PEG-PCL5930-PEI/siRNA	65.13	67.22	1.032	1383000	113.2
PEG-PCL8636-PEI/siRNA	68.63	72.82	1.061	1682000	99.3

replacement. On the other hand, this phenomenon can be explained by decreased N_{agg} (Table 4) and increased shielding of PEI charges by dense PEG shells of micellar assemblies. The structural differences have obvious effect on their drug loading properties.

Transmission electron micrographs (Supporting Information Fig. S11) concluded uniform size dispersion and spherical shape of assemblies. The blank assemblies produced by PEG-PCL8636-PEI showed dense cores and thin coronas due to the looped hydrophobic PCLs, while the PEG-PCL2945-PEI micellar assemblies had loose cores and thick shells originating from linear chain structure.

3.5. Static light scattering (SLS) for structure analysis of both blank and drug-loaded assemblies

SLS was performed to further elucidate the structure of both blank and drug-loaded assemblies. Importantly, R_g/R_h (R_g is radius of gyration determined by SLS and R_h is hydrodynamic radius measured by DLS) can be used to indicate structure of the assemblies, which R_g/R_h of flexible coils is about 1.5, R_g/R_h of core−shell spherical morphology is about 1.0 and R_g/R_h of uniform sphere is about 0.77[41]. The greater value of R_g/R_h implies loose structure while decreased R_g/R_h verifies compact formation.

The structural parameters were summarized in Table 4. As can be seen from results, average 60−90 triblock copolymers assembled into core−shell spherical structure. The assemblies' sizes changed with N_{agg} for PEG-PCL1947-PEI, PEG-PCL4006-PEI, PEG-PCL5930-PEI, which self-assembled into micelle-like structure (Fig. 4B). However, PEG-PCL8636-PEI did not exhibit the same trend due to different particle-like structure (Fig. 4C). The compact hydrophobic core extended sizes but decreased N_{agg}. Additionally, the smallest size of PEG-PCL4006-PEI corresponding to the lowest N_{agg} and the minimum R_g/R_h should attribute to the balanced hydrophilic/hydrophobic ratio, also applying to drug loaded assemblies, which implies stable structure and the lowest free energy.

After encapsulating hydrophobic DTX, the core−shell spherical structure remained unchanged. The N_{agg} of DTX-loaded assemblies were all decreased whereas sizes increased compared to blank ones. This phenomenon may result from DTX loading at hydrophobic core swell the structure consequently decreasing aggregation number[42] (Fig. 4D). The slightly decreased R_g/R_h indicated assemblies more ordered because DTX brought the additional hydrophobic force to stabilize the structure. After complexing with siRNA, the increased N_{agg} and sizes demonstrated siRNA may absorb more triblock copolymers to reassembly (Fig. 4E). The further reduced R_g/R_h suggested the electrostatic attraction between siRNA and PEI replaced the electrostatic repulsion among cationic chains resulting in increased aggregation number.

4. Discussion

To investigate the effects of block length and ratio on interfacial properties and self-assembly, a set of diblock PEG-PCL and triblock PEG-PCL-PEI copolymers with altered PCL lengths and fixed segments of PEG and PEI were synthesized (Table 1). The Mw 1900 Da of PEG was chosen because it could be excreted easily after PCL degradation *in vivo*[43]. PCL chains act as hydrophobic reservoirs entrapped with water-insoluble drugs[44]. Lower molecular weight (2500 Da) PEI used in our research exhibited reduced toxicity while maintained transmembrane transport and transfection efficiency[22]. Through mild reaction and effective purification, a library of copolymers were obtained and characterized to evaluate structure related properties intended for developing drug and gene vectors.

For diblock copolymers, PEG chains enter subphase and PCL chains anchor at the interface to form an ordered conformation (Fig. 2A). This is fit with previous studies on two-dimensional self-assembly of linear[27] and star-shaped PEG-PCL copolymers[45]. Although there are some surface pressure measurements about triblock copolymers[8,15], we first extend the interfacial and self-assembly study to PEG-PCL-PEI and investigate their inherent link. The triblock copolymers adopt vertical molecular orientation above the water (Fig. 2B). The hydrogen bonding between neighboring PEI and PEG chains contribute to film stability, leading to lower A_{min} and higher kink point compared to diblock copolymers (Fig. 1 and Table 2). Moreover, PEG-PCL8636-PEI with wide disparity hydrophilic/hydrophobic ratio has a special intermediate state, where two hydrophilic chains both enter the subphase and PCL chains forms hydrophobic loop (Fig. 2C). This is related to the flexible PCL chains are not sufficient to support vertical arrangement at lower pressure. Only at high surface pressure, one of hydrophilic chains is repelled out of water subphase, and PEG-PCL8636-PEI changes conformation to vertical state. The molecular arrangements (Fig. 2) were verified by AFM, changing subphase and measuring deformability of copolymers (Figs. S4−S6).

The relatively low CMC values of diblock and triblock copolymers (Fig. S7) promise their ability to form nano-assemblies in an aqueous environment and these nano-assemblies may maintain integrity even upon strong dilution in blood fluid[24,46]. Particle size is main parameters to influence quality, traffic and fate of vectors in the body. In general, particles smaller than 100 nm are capable to avoid rapid elimination by reticuloendothelial system (RES), and accumulate readily into the tumor site via enhanced permeability and retention (EPR) effect. The micelles of PEG1900-PCL1947 (~25 nm) among diblock copolymers and PEG1900-PCL4006-PEI2500 (~53 nm) in triblock copolymers have the smallest size as well as the lowest N_{agg} (Fig. 3 and Table 3) related to their harmonious hydrophilic−hydrophobic ratio. The fair ratio also helps the assembly form the most ordered structure corresponding to the minimum R_g/R_h (Table 4).

The self-assembly is triggered by phase separation, which PCL aggregates because of hydrophobic interactions and hydrophilic PEG and PEI surround hydrophobic core to form a shell[47]. The force balance among following three elements controls the aggregate morphology: the core chain stretching, the steric repulsions between corona chains, and the interfacial tension between core and solvent[10,48]. Therefore, the factor that contributes most to the force balance will have the biggest influence on assembly and thus various properties including block copolymer composition, ratio of hydrophilic to hydrophobic chain length will determine the final lowest energy structure. Trends in size as a function of copolymer concentration can be clarified by different assembly mechanisms, resulting in diverse structures[22] (Fig. 3C). The more hydrophilic copolymers assemble into smaller micellar-like structures, which hydrophilic chains governing the formation by preventing the PCL aggregation and moderating copolymer agglomeration (Fig. 4B). As to more hydrophobic copolymers PEG-PCL8636-PEI, looped PCL chains precipitate into compact core and copolymers form larger particular assemblies (Fig. 4C). The geometry of copolymer unimers correspond to distinct structural architectures, which linear polymeric blocks constitutes micelle phase while hydrophobic chains with higher curvature aggregate into particles. The different trends between sizes and N_{agg} for micellar and particular assemblies have also proved their architectural differences (Table 4). Assembly structures were elucidated by DLS, SLS, TEM and these structural differences between hydrophilic and hydrophobic copolymers have a profound correlation and impact on drug incorporation.

PEG-PCL8636-PEI had less DTX encapsulation compared to PEG-PCL4006-PEI (Table S4). This phenomenon may attribute to the high density of looped PCL chains leaving no enough space for drug loading in the interior. Another reason reported results from longer PCL chains tend to crystallize, which is not desirable for hydrophobic drug encapsulation[49,50]. Chemical modifications by introducing functional groups have been employed to make an amorphous core and improve drug load[17]. Additionally, conjugation of DTX onto PCL chains may provide extra interactions and favorable docking sites to achieve increased DTX incorporation[48]. The diversity in formation and structure also has impact on genetic condensation and anti-anion ability of copolymers (Fig. S9 and Fig. 5C). Block copolymers with a high hydrophilic ratio are generally favored to form larger area per corona chain and these dense PEG shells may shield positive charge. Encapsulating hydrophobic DTX or loading negatively charged siRNA did not change core−shell spherical structure, but made assemblies more compact than blank ones indicated by decreased R_g/R_h (Table 4). Hydrophobic DTX loading at the interior core bring additional hydrophobic interaction to stabilize assemblies. Moreover, electronegative hydrophilic siRNA located in the outer ring neutralize part of Coulomb repulsion to form more structured assemblies. Since the hydrophobic force is usually weak in blank assemblies, and drug encapsulation may introduce new forces to increase stability and retain integrity[41]. The DTX-loaded assemblies could prevent drug leakage in blood stream and reduce side effects. Meanwhile, PEG-PCL-PEI/siRNA complex can protect siRNA from degradation in systemic circulation. Upon accumulating in the tumor site, the drug-loaded assemblies release hydrophobic chemotherapeutics and gene drugs in sustained manner.

5. Conclusions

In summary, length ratio of hydrophilic/hydrophobic segments and block constituent have important impact on copolymers' interfacial properties and self-assembly formation. In this report, more hydrophilic copolymers (PCL<8636) formed vertical arrangement at the interface and then self-assembled into micellar structure in solution. Whereas, hydrophobic chains (PCL = 8636) adopted intermediate state at lower surface pressure and aggregated into particular-like structure in bulk. The structural architecture of copolymer chains are consistent in air/water interface and solution. Our study provides fundamental understanding about tailoring appropriate constituent ratio for obtaining desired molecular arrangement and nanoscale carrier. These factors have obvious effects on self-assembly's sizes, drug incorporation and stability. The micellar self-assemblies encapsulated more hydrophobic chemotherapeutics but did not condense nucleic acids well. On the contrary, particular-like structures condensed nucleic acids well but loaded less DTX. Systematic approaches investigated in this work provide insights on optimizing drug delivery system. This research reveals that the copolymer composition as key parameter is intrinsically linked to properties and nanostructure both at the air/water interface and in self-assembly.

Acknowledgments

We would like to acknowledge the NSFC (Nos. 81673365, 81973258 and 81473156, China), and the Fangzheng Foundation (China) for funding of the work. The authors also thank Prof. Xinjing Tang from State Key Laboratory of Natural and Biomimetic Drugs, School of Pharmaceutical Sciences, Peking University (Beijing, China) for his kind support for copolymer synthesis.

Author contributions

Ji Li was responsible for conceptualization, methodology, investigation, formal analysis, and writing original draft. Yitian Du was responsible for methodology, investigation, and formal analysis. Haitao Su and Shixuan Cheng were responsible for investigation and formal analysis. Yanxia Zhou was responsible for conceptualization, methodology, and resources. Yiguang Jin was responsible for review, editing, and supervision. Xian-Rong Qi was responsible for conceptualization, review, editing, supervision and funding acquisition.

Conflicts of interest

The authors declare no competing financial interest or other conflicts of interest.

Appendix A. Supporting information

Supporting data to this article can be found online at https://doi.org/10.1016/j.apsb.2020.01.006.

References

1. Priestley RD, Ellison CJ, Broadbelt LJ, Torkelson JM. Structural relaxation of polymer glasses at surfaces, interfaces, and in between. *Science* 2005;**309**:456−9.
2. Berret JF, Schonbeck N, Gazeau F, El Kharrat D, Sandre O, Vacher A, et al. Controlled clustering of superparamagnetic nanoparticles using block copolymers: design of new contrast agents for magnetic resonance imaging. *J Am Chem Soc* 2006;**128**:1755−61.
3. Bronstein LM, Chernyshov DM, Timofeeva GI, Dubrovina LV, Valetsky PM, Khokhlov AR. Polystyrene-*block*-poly(ethylene oxide) micelles in aqueous solution. *Langmuir* 1999;**15**:6195−200.
4. Tan BH, Hussain H, Chaw KC, Dickinson GH, Gudipati CS, Birch WR, Teo SL, et al. Barnacle repellent nanostructured surfaces formed by the self-assembly of amphiphilic block copolymers. *Polym Chem* 2010;**1**:276−9.
5. Li C, Wang J, Wang Y, Gao H, Wei G, Huang Y, et al. Recent progress in drug delivery. *Acta Pharm Sin B* 2019;**6**:1145−62.
6. Allen C, Han J, Yu Y, Maysinger D, Eisenberg A. Polycaprolactone-*b*-poly(ethylene oxide) copolymer micelles as a delivery vehicle for dihydrotestosterone. *J Control Release* 2000;**63**:275−86.
7. Park HW, Choi J, Ohn K, Lee H, Kim JW, Won YY. Study of the air-water interfacial properties of biodegradable polyesters and their block copolymers with poly(ethylene glycol). *Langmuir* 2012;**28**:11555−66.
8. Busse K, Peetla C, Kressler J. Water surface covering of fluorinated amphiphilic triblock copolymers: surface pressure-area and X-ray reflectivity investigations. *Langmuir* 2007;**23**:6975−82.
9. Zhang J, Wang LQ, Wang H, Tu K. Micellization phenomena of amphiphilic block copolymers based on methoxy poly(ethylene glycol) and either crystalline or amorphous poly(caprolactone-*b*-lactide). *Biomacromolecules* 2006;**7**:2492−500.
10. Fairley N, Hoang B, Allen C. Morphological control of poly(ethylene glycol)-*block*-poly(epsilon-caprolactone) copolymer aggregates in aqueous solution. *Biomacromolecules* 2008;**9**:2283−91.
11. Ge A, Wu H, Darwish TA, James M, Osawa M, Ye S. Structure and lateral interaction in mixed monolayers of dioctadecyldimethylammonium chloride (DOAC) and stearyl alcohol. *Langmuir* 2013;**29**:5407−17.
12. Jin Y, Wang S, Tong L, Du L. Rational design of didodecyldimethylammonium bromide-based nanoassemblies for gene delivery. *Colloids Surfaces B Biointerfaces* 2015;**126**:257−64.
13. Mostert AB, Davy KJ, Ruggles JL, Powell BJ, Gentle IR, Meredith P. Gaseous adsorption in melanins: hydrophilic biomacromolecules with high electrical conductivities. *Langmuir* 2010;**26**:412−6.
14. Abraham T, Schooling SR, Beveridge TJ, Katsaras J. Monolayer film behavior of lipopolysaccharide from *Pseudomonas aeruginosa* at the air-water interface. *Biomacromolecules* 2008;**9**:2799−804.
15. Fuchs C, Hussain H, Schwieger C, Schulz M, Binder WH, Kressler J. Molecular arrangement of symmetric and non-symmetric triblock copolymers of poly(ethylene oxide) and poly(isobutylene) at the air/water interface. *J Colloid Interface Sci* 2015;**437**:80−9.
16. Li Destri G, Gasperini AA, Konovalov O. The link between self-assembly and molecular conformation of amphiphilic block copolymers monolayers at the air/water interface: the spreading parameter. *Langmuir* 2015;**31**:8856−64.
17. Yan J, Ye Z, Chen M, Liu Z, Xiao Y, Zhang Y, et al. Fine tuning micellar core-forming block of poly(ethylene glycol)-*block*-poly(-epsilon-caprolactone) amphiphilic copolymers based on chemical modification for the solubilization and delivery of doxorubicin. *Biomacromolecules* 2011;**12**:2562−72.
18. Deng X, Yin Z, Zhou Z, Wang Y, Zhang F, Hu Q, et al. Carboxymethyl dextran-stabilized polyethylenimine-poly(epsilon-caprolactone) nanoparticles-mediated modulation of microRNA-34a expression *via* small-molecule modulator for hepatocellular carcinoma therapy. *ACS Appl Mater Interfaces* 2016;**8**:17068−79.
19. Wyman IW, Liu G. Micellar structures of linear triblock terpolymers: three blocks but many possibilities. *Polymer* 2013;**54**:1950−78.
20. Deschenes L, Bousmina M, Ritcey AM. Micellization of PEO/PS block copolymers at the air/water interface: a simple model for predicting the size and aggregation number of circular surface micelles. *Langmuir* 2008;**24**:3699−708.
21. James J, Ramalechume C, Mandal AB. Two-dimensional surface properties of PEO-PPO-PEO triblock copolymer film at the air/water interface in the absence and presence of Tyr-Phe dipeptide, Val-Tyr-Val tripeptide, SDS and stearic acid. *Colloids Surfaces B Biointerfaces* 2011;**82**:345−53.
22. Endres TK, Beck-Broichsitter M, Samsonova O, Renette T, Kissel TH. Self-assembled biodegradable amphiphilic PEG-PCL-lPEI triblock copolymers at the borderline between micelles and nanoparticles designed for drug and gene delivery. *Biomaterials* 2011;**32**:7721−31.
23. Liu Y, Samsonova O, Sproat B, Merkel O, Kissel TH. Biophysical characterization of hyper-branched polyethylenimine-*graft*-polycaprolactone-*block*-mono-methoxyl-poly(ethylene glycol) copolymers (hy-PEI-PCL-mPEG) for siRNA delivery. *J Control Release* 2011;**153**:262−8.
24. Jiao X, Yu Y, Meng J, He M, Zhang CJ, Geng W, et al. Dual-targeting and microenvironment-responsive micelles as a gene delivery system to improve the sensitivity of glioma to radiotherapy. *Acta Pharm Sin B* 2019;**9**:381−96.
25. Wang AT, Liang DS, Liu YJ, Qi XR. Roles of ligand and TPGS of micelles in regulating internalization, penetration and accumulation against sensitive or resistant tumor and therapy for multidrug resistant tumors. *Biomaterials* 2015;**53**:160−72.
26. Qin B, Chen Z, Jin W, Cheng K. Development of cholesteryl peptide micelles for siRNA delivery. *J Control Release* 2013;**172**:159−68.
27. Joncheray TJ, Denoncourt KM, Meier MA, Schubert US, Duran RS. Two-dimensional self-assembly of linear poly(ethylene oxide)-*b*-poly(epsilon-caprolactone) copolymers at the air-water interface. *Langmuir* 2007;**23**:2423−9.
28. Kim SH, Tan JP, Nederberg F, Fukushima K, Colson J, Yang C, et al. Hydrogen bonding-enhanced micelle assemblies for drug delivery. *Biomaterials* 2010;**31**:8063−71.
29. Kellner BMJ, Cadenhead DA. Monolayer studies of methyl hydroxyhexadecanoates. *Chem Phys Lipids* 1979;**23**:41−8.
30. Dunne LJ, Bell GM. Theory of cooperative phenomena in monolayers of hydroxyhexadecanoic acid isomers. *J Chem Soc Faraday Trans* 1980;**76**:431−40.
31. Lee H, Son SH, Sharma R, Won YY. A discussion of the pH-dependent protonation behaviors of poly(2-(dimethylamino)ethyl methacrylate) (PDMAEMA) and poly(ethylenimine-ran-2-ethyl-2-oxazoline) (P(EI-r-EOz)). *J Phys Chem B* 2011;**115**:844−60.
32. Xie D, Rezende CA, Liu G, Pispas S, Zhang G, Lee LT. Effect of hydrogen-bonding complexation on the interfacial behavior of poly (isoprene)-*b*-poly(ethylene oxide) and poly(isoprene)-*b*-poly(acrylic acid) Langmuir monolayers. *J Phys Chem B* 2009;**113**:739−44.
33. Yue Z, You Z, Yang Q, Lv P, Yue H, Wang B, et al. Molecular structure matters: PEG-*b*-PLA nanoparticles with hydrophilicity and deformability demonstrate their advantages for high-performance delivery of anti-cancer drugs. *J Mater Chem B* 2013;**1**:3239−47.
34. Xu L, Zhang Z, Wang F, Xie D, Yang S, Wang T, et al. Synthesis, characterization, and self-assembly of linear poly(ethylene oxide)-*block*-poly(propylene oxide)-*block*-poly(epsilon-caprolactone) (PEO-PPO-PCL) copolymers. *J Colloid Interface Sci* 2013;**393**:174−81.

35. Guo X, Wang L, Duval K, Fan J, Zhou S, Chen Z. Dimeric drug polymeric micelles with acid-active tumor targeting and FRET-traceable drug release. *Adv Mater* 2018;**30**. 1705436.
36. Rabanel JM, Faivre J, Tehrani SF, Lalloz A, Hildgen P, Banquy X. Effect of the polymer architecture on the structural and biophysical properties of PEG-PLA nanoparticles. *ACS Appl Mater Interfaces* 2015;**7**:10374−85.
37. Yang Y, Hua C, Dong CM. Synthesis, self-assembly, and *invitro* doxorubicin release behavior of dendron-like/linear/dendron-like poly(epsilon-caprolactone)-*b*-poly(ethylene glycol)-*b*-poly(epsilon-caprolactone) triblock copolymers. *Biomacromolecules* 2009;**10**:2310−8.
38. Wang F, Bronich TK, Kabanov AV, Rauh RD, Roovers J. Synthesis and characterization of star poly(epsilon-caprolactone)-*b*-poly(-ethylene glycol) and poly(L-lactide)-*b*-poly(ethylene glycol) copolymers: evaluation as drug delivery carriers. *Bioconjug Chem* 2008;**19**:1423−9.
39. Li J, Yu X, Wang Y, Yuan Y, Xiao H, Cheng D, et al. A reduction and pH dual-sensitive polymeric vector for long-circulating and tumor-targeted siRNA delivery. *Adv Mater* 2014;**26**:8217−24.
40. Liu Y, An S, Li J, Kuang Y, He X, Guo Y, et al. Brain-targeted co-delivery of therapeutic gene and peptide by multifunctional nanoparticles in Alzheimer's disease mice. *Biomaterials* 2016;**80**:33−45.
41. Wang J, Xing X, Fang X, Zhou C, Huang F, Wu Z, et al. Cationic amphiphilic drugs self-assemble to the core-shell interface of PEGylated phospholipid micelles and stabilize micellar structure. *Philos Trans A Math Phys Eng Sci* 2013;**371**:20120309.
42. Akiba I, Terada N, Hashida S, Sakurai K, Sato T, Shiraishi K, et al. Encapsulation of a hydrophobic drug into a polymer-micelle core explored with synchrotron SAXS. *Langmuir* 2010;**26**:7544−51.
43. Li Y, Qi XR, Maitani Y, Nagai T. PEG-PLA diblock copolymer micelle-like nanoparticles as all-*trans*-retinoic acid carrier: *in vitro* and *in vivo* characterizations. *Nanotechnology* 2009;**20**. 055106.
44. Liu Y, Steele T, Kissel TH. Degradation of hyper-branched poly (ethylenimine)-*graft*-poly(caprolactone)-*block*-monomethoxyl-poly(ethylene glycol) as a potential gene delivery vector. *Macromol Rapid Commun* 2010;**31**:1509−15.
45. Joncheray TJ, Denoncourt KM, Mathieu C, Meier MA, Schubert US, Duran RS. Langmuir and Langmuir−Blodgett films of poly(ethylene oxide)-*b*-poly(epsilon-caprolactone) star-shaped block copolymers. *Langmuir* 2006;**22**:9264−71.
46. Zheng M, Librizzi D, Kılıç A, Liu Y, Renz H, Merkel OM, et al. Enhancing *in vivo* circulation and siRNA delivery with biodegradable polyethylenimine-*graft*-polycaprolactone-*block*-poly(ethylene glycol) copolymers. *Biomaterials* 2012;**33**:6551−8.
47. Kim BH, Kim JY, Kim SO. Directed self-assembly of block copolymers for universal nanopatterning. *Soft Matter* 2013;**9**:2780−6.
48. Mikhail AS, Allen C. Poly(ethylene glycol)-*b*-poly(epsilon-caprolactone) micelles containing chemically conjugated and physically entrapped docetaxel: synthesis, characterization, and the influence of the drug on micelle morphology. *Biomacromolecules* 2010;**11**:1273−80.
49. Shuai X, Ai H, Nasongkla N, Kim S, Gao J. Micellar carriers based on block copolymers of poly(epsilon-caprolactone) and poly(ethylene glycol) for doxorubicin delivery. *J Control Release* 2004;**98**:415−26.
50. Zhang W, Li Y, Liu L, Sun Q, Shuai X, Zhu W, et al. Amphiphilic toothbrushlike copolymers based on poly(ethylene glycol) and poly(epsilon-caprolactone) as drug carriers with enhanced properties. *Biomacromolecules* 2010;**11**:1331−8.